Journal of Materials Science: Materials in Electronics (2018) 29:7701–7706
https://doi.org/10.1007/s10854-018-8765-1

Investigation on structure and thermoelectric properties in p-type $Bi_{0.48}Sb_{1.52}Te_3$ via PbTe incorporating

Shaojun Liang[1,2] · Jingtao Xu[2] · Hongxiang Wang[2] · Xiaojian Tan[2] · Guo-Qiang Liu[2] · Hezhu Shao[2] · Bo Yu[2] · Song Yue[1] · Jun Jiang[2]

Received: 9 January 2018 / Accepted: 12 February 2018 / Published online: 14 February 2018

Abstract
Bismuth telluride alloys are the most commercially used thermoelectric materials. Herein, $Bi_{0.48}Sb_{1.52}Te_3 + x$ wt% PbTe ($x = 0$, 0.05, 0.1, and 0.15) composites have been prepared by the zone-melting method. The microstructure and thermoelectric properties of the composites are investigated. It is found that PbTe addition could effectively improve the electrical properties of $Bi_{0.48}Sb_{1.52}Te_3$. As a result, a very large power factor of 55.5 μW cm^{-1} K^{-2} is achieved at 300 K for $x = 0.05$. Compared with the matrix, the largest figure of merit *ZT* for the composites shows slight enhancement, and the average figure of merit ZT_{ave} is obviously improved. This work indicated that a trace amount of PbTe can effectively improve the thermoelectric performance of $Bi_{0.48}Sb_{1.52}Te_3$.

1 Introduction

Thermoelectric materials have attracted extensive attention in the past decades due to their potential applications in direct thermal-to-electrical energy conversion without hazardous liquids, moving parts or greenhouse emissions [1–3]. The thermoelectric conversion efficiency is mainly determined by the dimensionless figure of merit *ZT*. *ZT* is defined as $ZT = \sigma\alpha^2 T/\kappa$, where α is the Seebeck coefficient, σ is the electrical conductivity, T is the absolute temperature, and κ is the total thermal conductivity containing both the carrier contribution κ_e and phonon contribution κ_l. Increasing the power factor $(\sigma\alpha^2)$ by energy band engineering and reducing κ by introducing additional phonon scattering are two common methods to improve the conversion efficiency of thermoelectric [4–10].

Bismuth telluride and its alloys (BiSbTe) are one of the most important thermoelectric materials near room temperature as so far. In recent years, several methods and techniques can be adopted to raise the *ZT* values of bismuth telluride based alloys such as microwave assisted method [11], hot pressing [12], mechanical alloying [13], spark plasma sintering [14, 15], magnetron sputtering [16] or by doping them with certain materials which can tune its properties [17]. Nanocomposite has been considered as a promising way to improve *ZT* by synergistically tuning the electrical and the thermal properties at the same time. ZnAlO, graphene, WSe_2 and silver have been reported to form effective nanoinclusions in Bi_2Te_3-based alloys, and improve their TE performance [8, 9, 18, 19]. For example, Zhao et al. reported that the addition of SiC nanopowders resulted in a remarkable decrease in thermal conductivity and improvement of mechanical properties of Bi_2Te_3-based alloys [20].

Lead telluride (PbTe) is one of the best materials used in thermoelectric generators operating at intermediate temperatures (450–800 K) [21]. This compound shows a larger band gap (0.3 eV) than bismuth telluride (0.13 eV) [22, 23], and low thermal conductivity. Better thermoelectric performance may be expected in bismuth telluride combined with PbTe. In this work, we prepare the BiSbTe alloys with additional PbTe using the zone melting (ZM) method. As

✉ Jingtao Xu
xujingtao@nimte.ac.cn

✉ Song Yue
ysongx50@163.com

✉ Jun Jiang
jjun@nimte.ac.cn

[1] Siyuan Laboratory, Guangzhou Key Laboratory of Vacuum Coating Technologies and New Energy Materials, Department of Physics, Jinan University, Guangzhou 510632, China

[2] Ningbo Institute of Materials Technology and Engineering, Chinese Academy of Sciences, Ningbo 315201, China

we will see, the PbTe addition improves the figure of merit in the medium temperature range.

2 Experimental section

Elements of bismuth (Bi, 99.999%), antimony (Sb, 99.999%), tellurium (Te, 99.999%), and PbTe (prepared by a melting method) were used for the preparation of the samples without further purifying. PbTe was directly prepared by melting Pb and Te. Then $Bi_{0.48}Sb_{1.52}Te_3 + x$ wt% PbTe samples ($x = 0$, 0.05, 0.1 and 0.15) were prepared by ZM. The starting materials were weighted and sealed into evacuated quartz tubes, and then heated at 1173 K for 30 min in a rocking furnace to ensure homogeneity. After naturally cooling to room temperature, the alloys were grown via the ZM method at temperatures of 993 K with a growth speed of 25 mm h^{-1}. Bars of 2 mm × 2 mm × 11 mm and discs of Φ 10 mm × 1.5 mm were cut from the samples along their growth direction to measure their electrical and thermal transport properties, respectively.

Phase structure of the samples was characterized by X-ray diffraction (XRD, Bruker AXS) using Cu K_α radiation ($\lambda = 1.5406$ Å). Microstructure was characterized by the field emission scanning electron microscopy (FESEM, Hitachi S4800). Electrical conductivity and Seebeck coefficient were measured by using a four-point probe method (ZEM-3). Thermal conductivity was calculated from the specific heat C_p, the thermal diffusivity λ, and the density ρ, using the equation $\kappa = C_p \lambda \rho$. Thermal diffusivity was measured by a laser flash method (NETZSCH LFA-457), and specific heat was a differential scanning calorimeter (Shimdzu DSC-50, Japan). The Hall coefficient R_H was measured by a physical property measurement system (Quantum Design, PPMS-9). Carrier concentration n and mobility μ were calculated by the relations $n = 1/eR_H$ and $\mu = \sigma R_H$.

3 Results and discussion

The powder XRD patterns of $Bi_{0.48}Sb_{1.52}Te_3 + x$ wt% PbTe composites ($x = 0$, 0.05, 0.1 and 0.15) are shown in Fig. 1a. All patterns are indexed to the BiSbTe structure with *R-3m* space group (JCPDS Card No.65-3674). No secondary peak of PbTe phase was observed in all compounds. This may be due to the tiny amount of PbTe. We use the Rietveld method to refine the lattice parameters of these $Bi_{0.48}Sb_{1.52}Te_3 + x$ wt% PbTe samples. As shown in Fig. 1b, with the increase of PbTe content, both a and c decrease monotonously, indicating that PbTe atoms may enter the sites of the BiSbTe lattice [24].

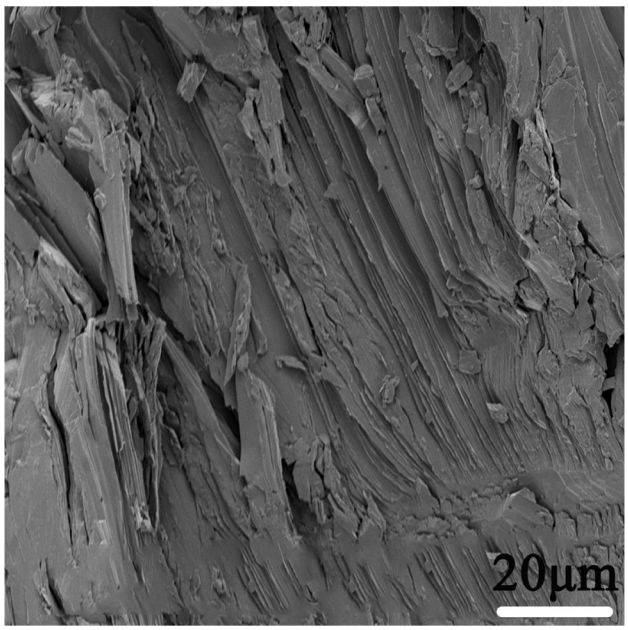

Fig. 2 SEM image of the fractured surfaces perpendicular to ZM direction for $Bi_{0.48}Sb_{1.52}Te_3 + 0.05$ wt% PbTe

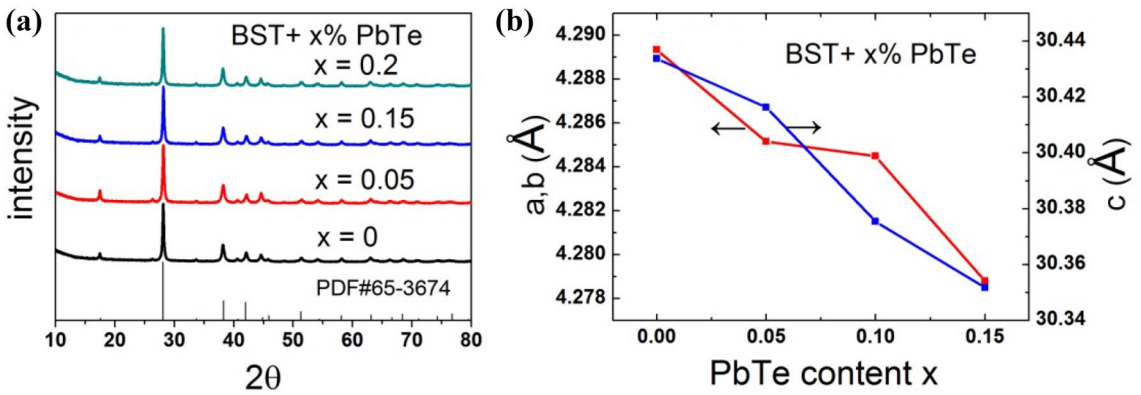

Fig. 1 **a** XRD patterns and **b** lattice parameters of $Bi_{0.48}Sb_{1.52}Te_3 + x$ wt% PbTe samples ($x = 0$, 0.05, 0.1 and 0.15)

Figure 2 displays the FESEM image of the fractured surfaces perpendicular to the ZM direction for BiSbTe + 0.05 wt% PbTe. The lamellar structure on the micron scale can be clearly observed. The grains show a size of several tens of micrometer and are preferentially oriented. It is well-known that the ZM method can fabricate polycrystalline samples with good textured degree.

Figure 3 presents the temperature dependence of the (a) electrical conductivity and (b) Seebeck coefficients of the $Bi_{0.48}Sb_{1.52}Te_3 + x$ wt% PbTe samples ($x = 0$, 0.05, 0.1 and 0.15). In Fig. 3a, the electrical conductivity σ decreases with increasing the temperature from 300 to 500 K for all the samples, showing a typical metallic behavior [25–27]. The conductivity σ increases monotonously with x and reaches its maximum value at $x = 0.15$. Especially at 300 K, the σ value significantly enhances from 1.29×10^3 Scm^{-1} for $x = 0$ to 2.09×10^3 Scm^{-1} for $x = 0.1$. These values are distinctly higher than 5.0×10^2 Scm^{-1} of PbTe–BiSbTe samples prepared by the solvothermal method [28]. The high value of electrical conductivity in the BiSbTe–PbTe composites should be attributed to the presence of Pb, which can introduce more hole carriers. To clarify the behavior of σ, we evaluated n and μ at room temperature. As shown in Table 1, the room temperature carrier concentration n is in the range of $3.37–5.56 \times 10^{19}$ cm^{-3}. Clearly, it is observed that PbTe addition increases the carrier concentration. On the other hand, μ decreases moderately with increasing PbTe, from 238 $cm^2\ V^{-1}\ s^{-1}$ for $x = 0$ to 191 $cm^2\ V^{-1}\ s^{-1}$ for $x = 0.1$, which is consistent with previous reports. It can be attributed to the enhancement of defect scattering [29–31].

Figure 3b gives the Seebeck coefficient α of all the samples as a function of temperature. The positive values of the Seebeck coefficients indicate that all the samples are p-type conductive. The Seebeck coefficients increase with increasing the temperature initially and then decreases, which is consistent with the previous reports [18, 19, 31]. The Goldsmid–Sharp band gap $E_g = 2e\alpha_{max}T(\alpha_{max})$ can be estimated from the maximum value of the Seebeck coefficient α_{max} and the corresponding temperature $T(\alpha_{max})$. The estimated values are about 0.17 eV for all samples which is similar to the literature report [25, 32] indicating that the introduction of PbTe has little impact on the band gap for the BiSbTe matrix. In contrast to the electrical conductivity σ, with the increasing PbTe content, the value of the Seebeck coefficients decreases. The highest Seebeck coefficient of 217 $\mu V\ K^{-1}$ is obtained at 405 K in the BiSbTe matrix. This value is similar to the results of the commercial zone melted BiSbTe [12, 19, 31], but smaller than those prepared from the chemical or spark plasma sintering methods [8, 28]. The peak of the Seebeck coefficient shifts to a higher temperature, which may be due to the suppression of the intrinsic excitation induced by the introduction of PbTe. The Seebeck coefficient can be calculated by

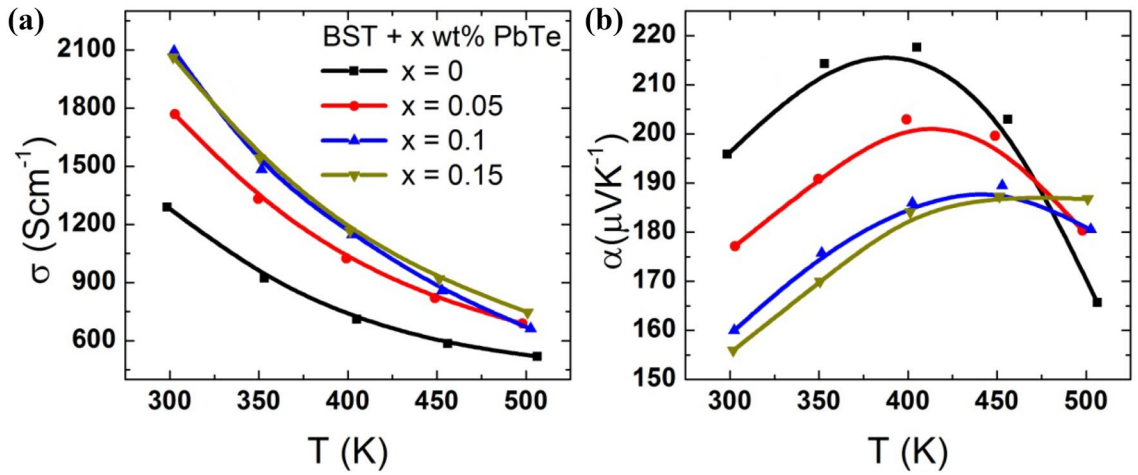

Fig. 3 Temperature dependence of the **a** electrical conductivity and **b** Seebeck coefficient for the $Bi_{0.48}Sb_{1.52}Te_3 + x$ wt% PbTe samples

Table 1 Hall coefficient R_H, carrier concentration n, mobility μ, Seebeck coefficient α and effective mass m^* of all the samples at room temperature

x	R_H (cm^3/C)	n (10^{19} cm^{-3})	μ ($cm^2\ V^{-1}\ s^{-1}$)	α ($\mu V\ K^{-1}$)	m^* (m_0)
0	0.185	3.37	238	196	0.93
0.05	0.120	5.23	211	177	1.12
0.1	0.091	6.84	191	160	1.21
0.15	0.112	5.56	232	156	1.03

$$\alpha = \frac{8\pi^2 k_B^{\ 2}}{3eh^2} m^* T \left(\frac{\pi}{3n}\right)^{2/3},$$

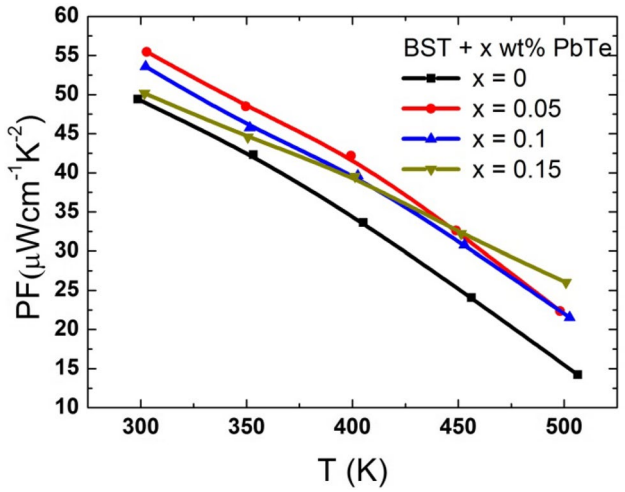

Fig. 4 Temperature dependence of the power factor for the $Bi_{0.48}Sb_{1.52}Te_3 + x$ wt% PbTe samples

where k_B, h, m^*, and n are Boltzmann constant, Planck constant, effective mass of carrier, and carrier concentration, respectively [8]. The effective mass of each sample is estimated and listed in Table 1. Such results are similar to those reported in previous work [33–35]. It can be seen that PbTe addition enhances the effective mass of carrier in the composites, compared to that in BiSbTe matrix.

Based on the measured σ and α results, the temperature dependence of the power factors $\left(\mathrm{PF} = \sigma\alpha^2\right)$ is summarized in Fig. 4. With the rising temperature, power factors for all the samples exhibit decrement. The maximum power factors of BiSbTe matrix is about 49 μW cm^{-1} K^{-2}. The power factors of all samples with PbTe incorporation are higher than the BiSbTe matrix and surpass 50 μW cm^{-1} K^{-2} at room temperature, which is attributed to the greatly improved electrical conductivity. When the addition is 0.05 wt%, the power factor reaches a maximum of 55 μW cm^{-1} K^{-2} at room temperature, which is 12% higher than that of BiSbTe. But with further increasing the content of PbTe, the power factor begins to decrease, due to the decrease of Seebeck coefficients (see Fig. 3b).

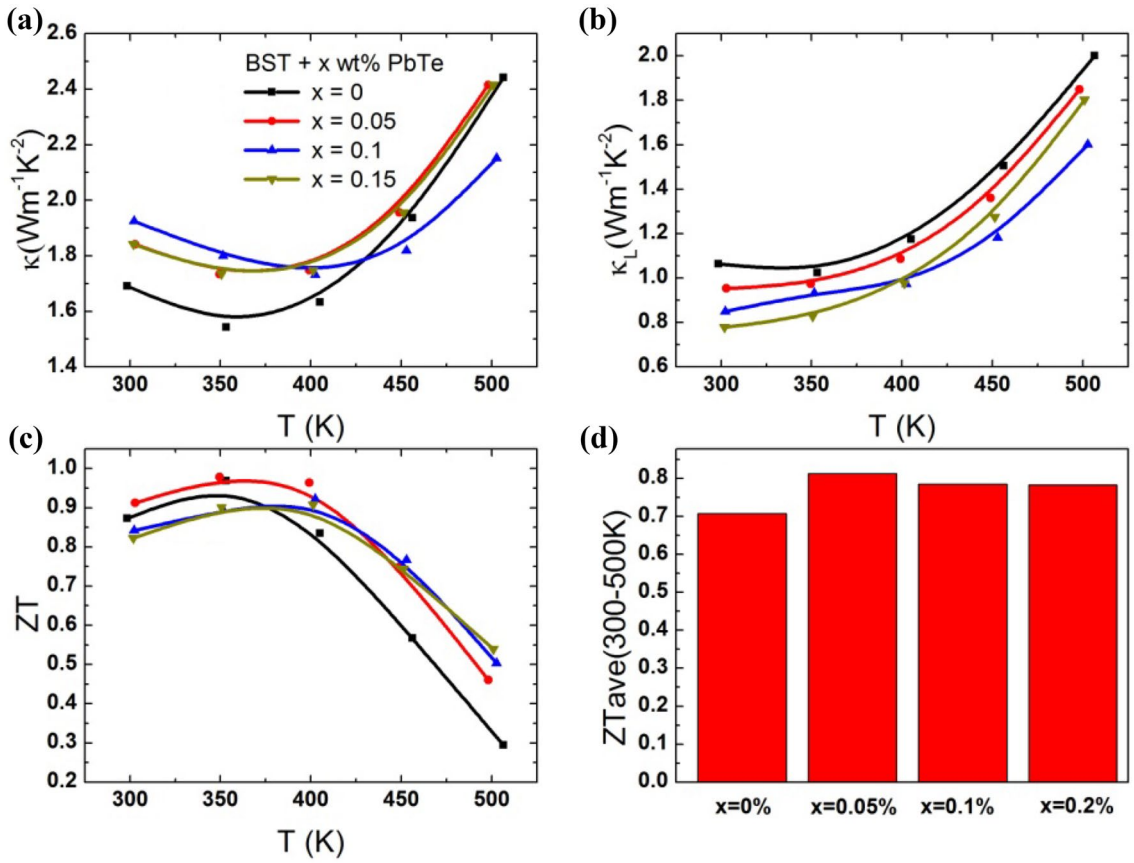

Fig. 5 Temperature dependence of the **a** total thermal conductivity, **b** lattice thermal conductivity, **c** figures of merit and **d** average *ZT* for the $Bi_{0.48}Sb_{1.52}Te_3 + x$ wt% PbTe samples

As shown in Fig. 5a, the temperature dependence of thermal conductivity for all samples first reduces due to the increasing phonon–phonon scattering, and then increases rapidly when further increasing testing temperature, which can be attributed to the bipolar thermal conductivity. The increasing n due to intrinsic excitation leads to a significant increase of the bipolar thermal conductivity. The minimum total thermal conductivity of BiSbTe matrix is about 1.54 W m^{-1} K^{-1}. The total thermal conductivity κ increases monotonously with increasing the content of PbTe over the entire temperature range. It is partly ascribed to the increase in the electronic thermal conductivity κ_e. The electronic thermal conductivity can be calculated from the formula $\kappa_e = L\sigma T$, where L is the Lorenz number. Here the Lorenz number L is roughly obtained by fitting the S to the reduced chemical potentials, which results in an L with a deviation of less than 10% as compared with a more rigorous single nonparabolic band and multiple band model calculation. The lattice thermal conductivity is then calculated by subtracting the electronic thermal conductivity from the total thermal conductivity, as shown in Fig. 5b. The reduction of lattice thermal conductivity can be observed clearly in the composites, indicating strong point defect phonon scattering by PbTe addition. When the content is 0.15 wt% the minimum lattice thermal conductivity is 0.83 W m^{-1} K^{-1} at 300 K.

The dimensionless thermoelectric figures of merit ZT of all bulk samples are calculated according to $ZT = \sigma\alpha^2 T/\kappa$. Figure 5c shows the temperature dependent ZT values of the BiSbTe + x wt% PbTe samples. It may seem that ZT for all samples increases with increasing temperature, reaches a maximum, and then decreases with further increasing temperature. The highest ZT value is about 1.0 at 350 K for the sample with $x = 0.05$. Comparing with the BiSbTe matrix, the composites have comparable ZT values before 375 K. Above this temperature, the ZT values of BiSbTe + x wt% PbTe composites are higher than the BiSbTe matrix, which are attributed to the improvement of power factors.

As known, the thermoelectric applications not only require a high peak ZT (ZT_{max}) but also require high ZTs in a wide temperature range. Thus, improving the average ZT (ZT_{ave}) is very beneficial for thermoelectric device applications. We calculated the average ZTs in the temperature range of 300–500 K and presented them in Fig. 5d. The PbTe-incorporated compounds show higher average ZT values, and the maximum ZT_{ave} is about 0.81 for $x = 0.05$.

4 Conclusions

$Bi_{0.48}Sb_{1.52}Te_3$ + x wt% PbTe ($x = 0$, 0.05, 0.1, and 0.15) composites were prepared by a ZM method. The results demonstrate that PbTe addition increases the electrical conductivity, and consequently the largest power factor is increased to 55.5 μW cm^{-1} K^{-2}. The improved electrical performance is mainly due to the increased carrier concentration. Compared with the $Bi_{0.48}Sb_{1.52}Te_3$ sample, the PbTe-incorporated samples have slightly higher peak ZT values, and a substantial enhancement of the average ZT values. The optimization of thermoelectric performance for $Bi_{0.48}Sb_{1.52}Te_3$ has been achieved by PbTe incorporating.

Acknowledgements This work was supported by the National Natural Science Foundation of China (11404350, 11404348, 51702334, and 11234012), the Zhejiang Provincial Science Foundation for Distinguished Young Scholars (LR16E020001), Natural Science Foundation of Zhejiang Province (LY18A040008 and LY18E020017), and the Ningbo Science and Technology Innovation Team (2014B82004).

References

1. G.J. Snyder, E.S. Toberer, Complex thermoelectric materials. Nat. Mater. **7**(2), 105–114 (2008)
2. W.G. Zeier, A. Zevalkink, Z.M. Gibbs, G. Hautier, M.G. Kanatzidis, G.J. Snyder, Thinking like a chemist: intuition in thermoelectric materials. Angew. Chem. Int. Ed. **55**(24), 6826–6841 (2016)
3. T. Zhu, Y. Liu, C. Fu, J.P. Heremans, J.G. Snyder, X. Zhao, Compromise and synergy in high-efficiency thermoelectric materials. Adv. Mater. 1605884 (2017)
4. W. Li, L. Zheng, B. Ge, S. Lin, X. Zhang, Z. Chen, Y. Chang, Y. Pei, Promoting SnTe as an eco-friendly solution for p-PbTe thermoelectric via band convergence and interstitial defects. Adv. Mater. 1605887 (2017)
5. S. Lin, W. Li, Z. Chen, J. Shen, B. Ge, Y. Pei, Tellurium as a high-performance elemental thermoelectric. Nat. Commun. **7**, 10287 (2016)
6. F. Yu, J. Zhang, D. Yu, J. He, Z. Liu, B. Xu, Y. Tian, Enhanced thermoelectric figure of merit in nanocrystalline Bi_2Te_3 bulk. J. Appl. Phys. **105**(9), 094303 (2009)
7. W. Xie, X. Tang, Y. Yan, Q. Zhang, T.M. Tritt, High thermoelectric performance BiSbTe alloy with unique low-dimensional structure. J. Appl. Phys. **105**(11), 113713 (2009)
8. C. Chen, D.W. Liu, B.P. Zhang, J.F. Li, Enhanced thermoelectric properties obtained by compositional optimization in p-Type $Bi_xSb_{2-x}Te_3$ fabricated by mechanical alloying and spark plasma sintering. J. Electron. Mater. **40**(5), 942–947 (2011)
9. T. Zhang, Q. Zhang, J. Jiang, Z. Xiong, J. Chen, Y. Zhang, W. Li, G. Xu, Enhanced thermoelectric performance in p-type BiSbTe bulk alloy with nanoinclusion of ZnAlO. Appl. Phys. Lett. **98**(2), 022104 (2011)
10. B. Poudel, Q. Hao, Y. Ma, Y. Lan, A. Minnich, B. Yu, X. Yan, D. Wang, A. Muto, D. Vashaee, X. Chen, High-thermoelectric performance of nanostructured bismuth antimony telluride bulk alloys. Science **320**(5876), 634–638 (2008)
11. J.P. Ge, Y.D. Li, Ultrasonic synthesis of nanocrystals of metal selenides and tellurides. J. Mater. Chem. **13**(4), 911–915 (2003)
12. J.J. Shen, Z.Z. Yin, S.H. Yang, C. Yu, T.J. Zhu, X.B. Zhao, Improved thermoelectric performance of p-type bismuth antimony telluride bulk alloys prepared by hot forging. J. Electron. Mater. **40**(5), 1095–1099 (2011)
13. J.Y. Yang, X.A. Fan, R.G. Chen, W. Zhu, S.Q. Bao, X.K. Duan, Consolidation and thermoelectric properties of n-type bismuth telluride based materials by mechanical alloying and hot pressing. J. Alloy. Compd. **416**(1), 270–273 (2006)

14. Z. Zhang, P.A. Sharma, E.J. Lavernia, N. Yang, Thermoelectric and transport properties of nanostructured Bi_2Te_3 by spark plasma sintering. J. Mater. Res. **26**(3), 475–484 (2011)
15. J. Jiang, L. Chen, S. Bai, Q. Yao, Q. Wang, Thermoelectric properties of textured p-type $(Bi,Sb)_2Te_3$ fabricated by spark plasma sintering. Scr. Mater. **52**(5), 347–351 (2005)
16. Y. Zhou, L. Li, Q. Tan, J.F. Li, Thermoelectric properties of Pb-doped bismuth telluride thin films deposited by magnetron sputtering. J. Alloy. Compd. **590**, 362–367 (2014)
17. K. Park, S.W. Nam, C.H. Lim, Thermoelectric properties of p-type $Bi_{0.5}Sb_{1.5}Te_3$ for solid-state cooling devices. Intermetallics **18**(9), 1744–1749 (2010)
18. D. Suh, S. Lee, H. Mun, S.H. Park, K.H. Lee, S.W. Kim, J.Y. Choi, S. Baik, Enhanced thermoelectric performance of $Bi_{0.5}Sb_{1.5}Te_3$-expanded graphene composites by simultaneous modulation of electronic and thermal carrier transport. Nano Energy **13**, 67–76 (2015)
19. D. Xie, J. Xu, G. Liu, Z. Liu, H. Shao, X. Tan, J. Jiang, H. Jiang, Synergistic optimization of thermoelectric performance in p-type $Bi_{0.48}Sb_{1.52}Te_3$/graphene composite. Energies **9**(4), 236 (2016)
20. L.D. Zhao, B.P. Zhang, J.F. Li, M. Zhou, W.S. Liu, J. Liu, Thermoelectric and mechanical properties of nano-SiC-dispersed Bi_2Te_3 fabricated by mechanical alloying and spark plasma sintering. J. Alloy. Compd. **455**(1), 259–264 (2008)
21. T.J. Zhu, Y.Q. Liu, X.B. Zhao, Synthesis of PbTe thermoelectric materials by alkaline reducing chemical routes. Mater. Res. Bull. **43**(11), 2850–2854 (2008)
22. I.G. Austin, The optical properties of bismuth telluride. Proc. Phys. Soc. **72**(4), 545 (1958)
23. H. Köhler, Non-parabolicity of the highest valence band of Bi_2Te_3 from Shubnikov-de Haas effect. Phys. Status Solidi B **74**(2), 591–600 (1976)
24. F. Hao, P. Qiu, Q. Song, H. Chen, P. Lu, D. Ren, X. Shi, L. Chen, Roles of Cu in the enhanced thermoelectric properties in $Bi_{0.5}Sb_{1.5}Te_3$. Materials **10**(3), 251 (2017)
25. T. Zhang, J. Jiang, Y. Xiao, Y. Zhai, S. Yang, G. Xu, In situ precipitation of Te nanoparticles in p-type BiSbTe and the effect on thermoelectric performance. ACS Appl. Mater. Interface **5**(8), 3071–3074 (2013)
26. C. Jiang, X.A. Fan, B. Feng, J. Hu, Q. Xiang, G. Li, Y. Li, Z. He, Thermal stability of p-type polycrystalline Bi_2Te_3-based bulks for the application on thermoelectric power generation. J. Alloy. Compd. **692**, 885–891 (2017)
27. C. Zhang, M. de la Mata, Z. Li, F.J. Belarre, J. Arbiol, K.A. Khor, D. Poletti, B. Zhu, Q. Yan, Q. Xiong, Enhanced thermoelectric performance of solution-derived bismuth telluride based nanocomposites via liquid-phase Sintering. Nano Energy **30**, 630–638 (2016)
28. B. Xu, M.T. Agne, T. Feng, T.C. Chasapis, X. Ruan, Y. Zhou, H. Zheng, J.H. Bahk, M.G. Kanatzidis, G.J. Snyder, Y. Wu, Nanocomposites from solution-synthesized PbTe-BiSbTe nanoheterostructure with unity figure of merit at low-medium temperatures (500–600 K). Adv. Mater. **29**(10) (2017)
29. Q. Zhang, X. Ai, L. Wang, Y. Chang, W. Luo, W. Jiang, L. Chen, Improved thermoelectric performance of silver nanoparticles-dispersed Bi_2Te_3 composites deriving from hierarchical two-phased heterostructure. Adv. Funct. Mater. **25**(6), 966–976 (2015)
30. Z.J. Xu, L.P. Hu, P.J. Ying, X.B. Zhao, T.J. Zhu, Enhanced thermoelectric and mechanical properties of zone melted p-type $(Bi,Sb)_2Te_3$ thermoelectric materials by hot deformation. Acta Mater. **84**, 385–392 (2015)
31. Y. Xiao, G. Chen, H. Qin, M. Wu, Z. Xiao, J. Jiang, J. Xu, H. jiang, G. Xu, Enhanced thermoelectric figure of merit in p-type $Bi_{0.48}Sb_{1.52}Te_3$ alloy with WSe_2 addition. J. Mater. Chem. A **2**(22), 8512–8516 (2014)
32. L.P. Hu, T.J. Zhu, Y.G. Wang, H.H. Xie, Z.J. Xu, X.B. Zhao, Shifting up the optimum figure of merit of p-type bismuth telluride-based thermoelectric materials for power generation by suppressing intrinsic conduction. NPG Asia Mater. **6**(2), e88 (2014)
33. J. Li, Q. Tan, J.F. Li, D.W. Liu, F. Li, Z.Y. Li, M. Zou, K. Wang, BiSbTe-based nanocomposites with high ZT: the effect of SiC nanodispersion on thermoelectric properties. Adv. Funct. Mater. **23**(35), 4317–4323 (2013)
34. G. Zheng, X. Su, T. Liang, Q. Lu, Y. Yan, C. Uher, X. Tang, High thermoelectric performance of mechanically robust n-type $Bi_2Te_{3-x}Se_x$ prepared by combustion synthesis. J. Mater. Chem. A **3**(12), 6603–6613 (2015)
35. Z.J. Xu, L.P. Hu, P.J. Ying, X.B. Zhao, T.J. Zhu, Enhanced thermoelectric and mechanical properties of zone melted p-type (Bi, $Sb)_2$ Te_3 thermoelectric materials by hot deformation. Acta Mater. **84**, 385–392 (2015)